Journal of Biomedical Optics

SPIEDigitalLibrary.org/jbo

Mapping optical fluence variations in highly scattering media by measuring ultrasonically modulated backscattered light

Altaf Hussain
Khalid Daoudi
Erwin Hondebrink
Wiendelt Steenbergen

SPIE

Mapping optical fluence variations in highly scattering media by measuring ultrasonically modulated backscattered light

Altaf Hussain,* Khalid Daoudi, Erwin Hondebrink, and Wiendelt Steenbergen*
University of Twente, MIRA Institute for Biomedical Technology and Technical Medicine, Biomedical Photonic Imaging Group, P.O. Box 217, 7500 AE Enschede, The Netherlands

Abstract. Knowledge of the local optical fluence in biological tissue is of fundamental importance for biomedical optical techniques to achieve quantification. We report a method to noninvasively measure the local optical fluence in optically inhomogeneous scattering media. The concept is based on two aspects: the local tagging of light using ultrasonic modulation and the photon path reversibility principle. Our method has advantages over known computational-based fluence mapping techniques, for its purely experimental nature and without the requirement of prior knowledge of the optical properties of the medium. We provide a theoretical formalism and validation of the method with experiments in tissue-like phantoms. Further, we combine our method with photoacoustic imaging and compensate the photoacoustic signals for fluence variations in optically inhomogeneous media. [DOI: 10.1117/1.JBO.19.6.066002]

Keywords: tissue scattering; optical fluence mapping; ultrasound-modulated optical tomography; quantitative photoacoustic imaging; photoacoustic.

Paper 140015R received Jan. 9, 2014; revised manuscript received Apr. 19, 2014; accepted for publication May 7, 2014; published online Jun. 2, 2014; corrected Jun. 6, 2014.

1 Introduction

In recent years, optical techniques such as photoacoustic imaging (PAI),[1,2] ultrasound-modulated optical tomography,[3] fluorescence imaging,[4] and diffuse optical tomography (DOT)[5] have been employed with great success for imaging deep inside highly scattering biological tissue. Due to the scattering and absorbing nature of biological tissue, the optical fluence decays with the distance from the light source. As a result, the amount of light reaching a point away from the light source becomes unknown. The lack of information about local fluence prevents the above methods from achieving quantification. Currently, methods to estimate the fluence distribution in biological tissue are based on various theoretical models, each with their own respective drawbacks. It is known that the radiative transfer equation (RTE) accurately describes photon propagation in biological tissue.[6,7] However, solutions of RTE exist only for simple cases where the medium is infinite and homogeneous.[8] In media with dominant scattering compared to absorption, the fluence rate far from optical boundaries and the light source can be approximated using diffusion theory.[9] In more complex media, computational models are used to solve RTE under certain approximations,[10,11] including the most commonly used method—Monte Carlo simulations.[12] To estimate optical fluence in biological tissue using the above-mentioned techniques, exact knowledge of optical properties of the medium is required. Unfortunately, in real biological tissue, neither are the exact optical properties known, nor is the medium homogeneous, which limits the practicality of these methods. An experimental technique that vanquishes the aforementioned needs of a priori knowledge of the medium properties would be more practical.

Here, we present an experimental method to noninvasively measure local fluence in optically scattering media. The proposed method is based on local tagging of light using ultrasonic modulation[13] and subsequent detection of backscattered tagged photons. First, we describe a theoretical model and then experimentally validate the concept by comparing our noninvasively measured relative fluence in a tissue-like scattering medium with invasively measured fluence using an optical fiber. Next, to show the potential of our method to assist other biomedical optical techniques toward quantification, we demonstrate the case of PAI. We measured the local fluence in an optically heterogeneous medium containing several optical absorbers and used it to fluence-compensate PA signals. PAI is a promising high-resolution imaging modality, and it can benefit further from quantification by fluence compensation.[14] Several approaches based on computational models,[14–16] as well as experimental methods,[17] have been proposed to achieve this goal with moderate success. Intuitively, acousto-optics (AO) scans are related to the fluence rate;[3] however, no general strategy exists to apply it as a quantitative sensor of total optical fluence. Formerly, we have shown that combining PA and AO can yield fluence correction of PA signals.[18] The experiment involved two consecutive PA measurements by exciting the medium at two points, and a transmission mode AO measurement with the optodes coinciding with the PA excitation points. In that case, the results of both modalities are only meaningful if combined.[18] In this paper, we demonstrate that with a pure reflection mode approach, AO alone directly provides the fluence measurement.

*Address all correspondence to: Altaf Hussain, E-mail: a.hussain@utwente.nl; Wiendelt Steenbergen, E-mail: w.steenbergen@utwente.nl

2 Theory

The formalism of our theoretical model is based on photon path reversibility in scattering media.[18] Consider a scattering medium with an illumination point 1 on the surface and an internal point 2. On injection of light at point 1 with power P_1, the total power detected through an aperture with area A_2 and solid opening angle Ω_2 placed at point 2 can be written as $P_{1,2} = A_2\Omega_2 P_1 \Pr(1,2)$. Here, $\Pr(1,2)$ is the probability per unit area and per unit solid angle that a photon injected at point 1 will cross the aperture placed at point 2, following any possible trajectory. As a result of power $P_{1,2}$ at point 2, the fluence rate $\varphi_{1,2}$ is

$$\varphi_{1,2} = 4\pi P_1 \Pr(1,2). \tag{1}$$

gives rise to the detection of tagged photons within to the "tagging volume," considering a known fraction η (i.e., tagging efficiency) of the photons addressing this internal volume is tagged. Assuming an incoming fluence rate $\varphi_{1,2}$ and neglecting absorption in the tagging volume, the power of labeled/tagged photons reinjected into the medium is

$$P_{l,2} = \varphi_{1,2}\eta A_2 = 4\pi P_1 \Pr(1,2)\eta A_2, \tag{2}$$

where A_2 is the average effective frontal area of the tagging volume. Following the same reasoning as above, the internally injected stream of tagged photons at power $P_{l,2}$ gives rise to the detection of tagged photons within an area A_1 and solid opening angle Ω_1 at point 1, at a power

$$P_{l,1} = A_1\Omega_1 P_{l,2} \Pr(2,1) = 4\pi P_1 \Pr(1,2) \Pr(2,1)\eta A_2 A_1 \Omega_1. \tag{3}$$

Photon path reversibility gives $\Pr(1,2) = \Pr(2,1)$, and rearranging the expression for fluence $\varphi_{1,2}$ [Eq. (1)] and detected power of labeled photons $P_{l,1}$ [Eq. (3)], we obtain for local fluence rate $\varphi_{1,2}$ at point 2 in term of externally measured parameter $P_{l,1}$

$$\varphi_{1,2} = \sqrt{\frac{4\pi P_1}{\eta A_2 A_1 \Omega_1}}\sqrt{P_{l,1}}. \tag{4}$$

The above expression for local optical fluence contains the excitation parameter P_1; detection parameters Ω_1, A_1; parameters related to ultrasound focus A_2 and the interaction between light and ultrasound η; and the externally measurable quantity: power of tagged light $P_{l,1}$. The significance of Eq. (4) is that a pure reflection mode AO measurement gives a measure of the optical fluence inside the scattering medium without the requirement of a priori knowledge about the optical properties of the medium. Further detailed discussion about all the parameters in Eq. (4) is given in Secs. 3.2 and 5.

3 Materials and Methods

3.1 *Tissue-Mimicking Phantoms*

In total, three scattering tissue-mimicking phantoms of dimensions $3 \times 3 \times 3$ cm^3, namely A, B, and C, are used in experiments. Optical fluence measurement experiments are performed on phantoms A and B. Both samples are prepared using 3% agar gel and various concentrations of Intralipid (IL, 20% fat emulsion) leading to a range of reduced scattering coefficients (μ_s') to mimic optical scattering inhomogeneities, while the absorption is governed by water. Sample A is homogeneously scattering with $\mu_s' = 7.5$ cm^{-1}, whereas sample B consists of three different scattering layers, $0 \le x \le 0.9$ cm with $\mu_s' = 10$ cm^{-1}, $0.9 \le x \le 1.5$ cm with $\mu_s' = 6$ cm^{-1}, and $1.5 \le x \le 3$ cm with $\mu_s' = 15$ cm^{-1} [Fig. 1(a)].

Sample C is used for an experiment where PA signals are compensated for fluence variations. The sample consisted of two halves, with 4% IL (20% fat emulsion) concentration in one half and 7% in the other, having estimated $\mu_s' = 6$ cm^{-1} and $\mu_s' = 10$ cm^{-1}, respectively [Fig. 1(a)]. In each scattering half, three nylon tubes are embedded at depths of 4, 8, and 12 mm under the surface, mimicking blood vessels. The tubes having inner and outer diameters of 0.75 and 0.95 mm were filled with a solution of Ecoline (Royal Talens) in water having the absorption coefficient of $\mu_a = 9.31$ cm^{-1} at 532-nm wavelength.

3.2 *Experimental Measurement of Fluence*

In Sec. 2, we developed an analytical model Eq. (4) that relates the power of ultrasonically modulated light measured at the boundary of the scattering media to local fluence at an internal point. In experiments, we made use of ultrasonic modulation of light for tagging of light that addresses an region of interest (ROI) in a scattering medium. Since ultrasound waves exhibit a negligible scattering in comparison with light waves, it can be used to address a well-defined region deep inside the optically scattering medium with millimeter lateral and axial resolution. In order to use Eq. (4) in combination with the ultrasonic modulation of light to estimate the absolute local fluence, one must know the tagging efficiency η of the ultrasound and the effective frontal area A_2 of the US focus. The tagging efficiency η is the ratio of the US modulated light power leaving the focus to the total light power addressing the US focus, which is an unknown factor in Eq. (4). Therefore, for simplicity, we assume that the tagging efficiency η is independent of the local scattering property and the medium is acoustically homogeneous such that the effective frontal area A_2 of the US focus remains unchanged. These assumptions will be discussed further in Sec. 5. As a result, all the parameters under the first square root on the right-hand side of Eq. (4) can be merged into a single constant for a given experimental configuration. When the above assumptions are justified, Eq. (4) adopts the form $\varphi_{1,2} = \kappa\sqrt{P_{1,1}}$, where $P_{1,1}$ is the measured power of the backscattered ultrasonically modulated light.

There are several known methods to measure ultrasonically modulated light,[19–21] and fast detection methods[22,23] are being developed to overcome the tissue dynamics. In experiments presented here, we used a method based on the speckle contrast change for the detection of ultrasonically modulated light.[19] The speckle contrast ($C = \sigma/\langle I\rangle$) is the ratio of the standard deviation (σ) of the light intensity in the speckle pattern to the average light intensity. A perturbation, such as the presence of the US in the scattering media, causes the optical path length of photons interacting with it to change, which in turns blurs the speckle pattern. The change in speckle contrast (ΔC) between US ON and OFF states is related to the power of ultrasonically modulated light.[19] In a typical AO experiment, where short bursts of high-frequency (>1 MHz) ultrasound are used to modulate the light in diffused background, the fraction of US-modulated light is much smaller than unity.[19] In such an

AO experiment, the measured change in speckle contrast becomes approximately proportional to the power of ultrasonically modulated light.[19] Hence, the model Eq. (4) for estimating the fluence can be written as

$$\varphi_{1,2} = \kappa\sqrt{\Delta C}. \tag{5}$$

3.2.1 *Experimental setup*

Figure 1(b) depicts the schematic of the experimental setup to measure optical fluence in scattering media. Light from a single-mode CW laser (Verdi 6, Coherent, at 532 nm) is converted into pulses of 1 μs using an AO modulator driven by a dual-channel function generator (FG). The laser beam is directed onto the sample using a polarization beam splitter (PBS) through an aperture (diameter 5 mm). A CCD camera (GRAS-14S5M-C, 1384×1036) is placed behind the PBS to record the speckle patterns of diffuse light backscattered from the sample. The orientation of the PBS is such that it prevents the specularly reflected light from the surface of the sample to go onto the CCD. For local modulation of light, we send short (1 μs) intense ultrasound pulses ($\approx$1 MPa) into medium in synchronization with laser pulses. The pulses are generated using the second channel of aforementioned FG, which are then amplified with a radio-frequency amplifier (ENI; 350L) to drive the focused ultrasound transducer (Panametrics: V309 @ 5 MHz, $f = 20$ mm). The ultrasound transducer was aligned so that its focal point is in the illumination plane of the sample [Fig. 1(b)]. The laser pulse was delayed relative to ultrasound pulse so that at the instant of the laser pulse the ultrasound burst has reached the focal point of the transducer. The average light intensity incident on the sample was 24 mW cm^{-2} and exposure time of the CCD camera was set at 4 ms to acquire a speckle image.

3.2.2 *Measurement and validation procedure*

Change in speckle contrast ΔC in the backscattered light was measured at each US focus location. The US focus was scanned along the optical axis (x-axis) in the illumination plane of the sample; scanning was achieved using an automated translation stage (MTS25B-Z8). The measured change in speckle contrast ΔC as function of depth along the optical axis (x-axis) was then translated into local fluence using Eq. (5). At each US focus location, 15 measurements of ΔC were made and averaged to improve the signal-to-noise ratio.

In order to validate our approach to noninvasively measuring the local fluence, we invasively measured the local fluence at each US focus position using a multimode optical fiber (AFS, Core/cladding diameter: 400/440 μm) and the aforementioned CCD camera. The fiber was positioned along the optical axis (x-axis) and resided at the edge of the ultrasound focus as shown in Fig. 1(b). Precise positioning of the fiber was achieved using pulse-echo guidance, and the fiber was locked to the translation stage used for scanning the ultrasound focus. This allowed for a point-to-point comparison of noninvasively [using Eq. (5)] and invasively (with an optical fiber) measured fluence.

3.3 *Photoacoustic Imaging*

In this work, we demonstrate the importance and relevance of the proposed method to the biomedical imaging technique with an example. In PAI, the initial stress distribution σ_o as a response to locally absorbed energy is given as $\sigma_o = \Gamma\mu_a\varphi$, where Γ is the Grüneisen parameter, μ_a is the local absorption coefficient responsible for optical contrast, and φ is the local fluence. The fluence φ dependence needs to be eliminated from the above equation in order to directly relate the PA images to the optical absorption, which will lead to the most desired quantification.[14]

The schematic of the PA experimental setup is depicted in Fig. 1(c). A pulsed Nd:YAG laser (Quanta-Ray Lab-Series)

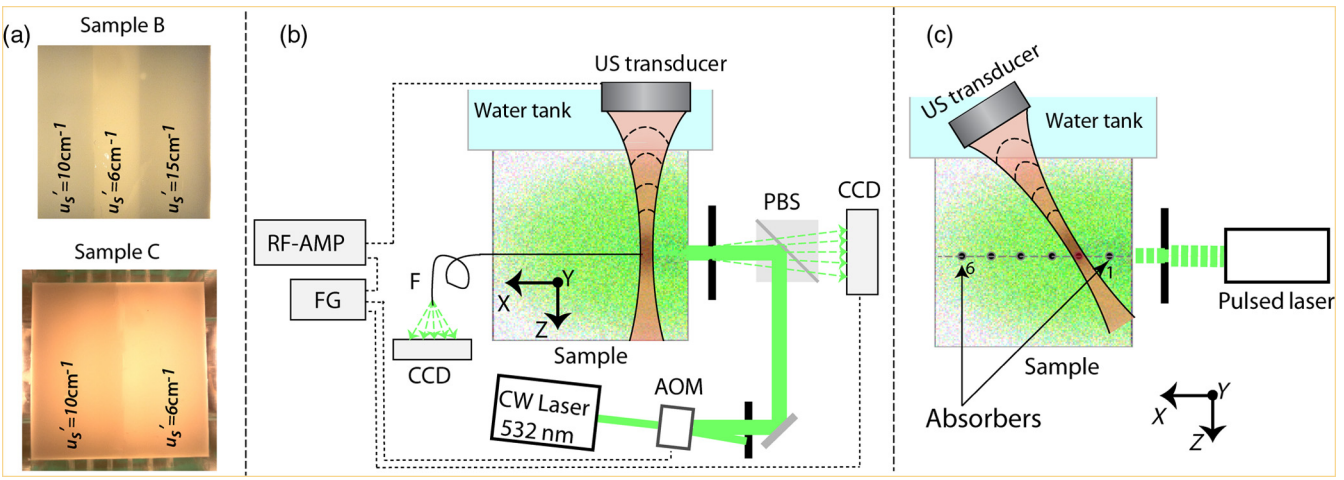

Fig. 1 (a) Photos of sample B (top view) showing three layers with different scattering levels and sample C (top view) showing two layers with different levels of scattering and three nylon tubes in each part containing absorbing solutions. (b) Experimental setup for measuring optical fluence: single-mode laser ($\lambda = 532$ nm). AOM, acousto optic light modulator; PBS, polarization beam splitter; US, ultrasound transducer; RF-Amp, radio-frequency power amplifier; FG, function generator; F, optical fiber. (c) PA experimental setup: pulsed laser ($\lambda = 532$ nm, pulse duration 5 ns) illuminating sample C through an aperture. PA signals are acquired using a single element focused US transducer followed by an amplifier and data acquisition system (not shown in schematic). Six absorbers embedded along the optical axis (x-axis).

emitting at 532-nm wavelength and delivering 10 mJ/pulse energy is used to excite the sample. The PA signals from the absorbers are measured with a single element focused ultrasound transducer (Panametrics: V310-su, Waltham, Massachusetts, 5 MHz), then amplified and acquired using a data acquisition system (Acqiris). The ultrasound transducer was oriented at approximately a 45-deg angle with the normal to the plane of the absorbers, in order to spatially resolve the tubes Fig. 1(c). By each absorbing tube being placed in the transducer focus, the PA response of the absorbers was measured. It also ensures that the effect of frequency-dependent attenuation and r^{-1} decay of the signal from each absorber is the same.

4 Results

4.1 *Optical Fluence Measurements*

Following the procedure described in Sec. 3.2.2, we measured the optical fluence noninvasively and invasively in samples A and B [Fig. 1(a)]. Figures 2(a) and 2(b) show the comparison of noninvasively and invasively measured optical fluence in a homogeneous sample A and inhomogeneous sample B versus the depth along the optical axis. The results on the optical fluence in Fig. 2 are normalized to the maximum value to eliminate the constant κ [Eq. (5)] for the noninvasive case, and the constant related to collection efficiency of optical fiber and detection efficiency of CCD camera for the invasive case. Figure 2 shows a good agreement between noninvasively and invasively measured fluence for the optically homogeneous as well as for the inhomogeneous sample B [Fig. 1(a)]. Since sample B was composed of three layers with different scattering coefficients, the decay in fluence with depth should present three slopes as a result of varying local effective attenuation coefficient in these regions. As expected, the results in Fig. 2(b) show both noninvasively (circles) and invasively (squares) measured fluence in sample B exhibiting three different slopes, and measurements are in mutual agreement in all three regions. However, inserting a fiber into the medium for invasive measurement of fluence might perturb the medium. To see the effect of this perturbation on the noninvasively measured fluence, we estimated the fluence using the noninvasive method twice—before and after the invasive measurements. The results did not show any significant difference, which confirms that the perturbation was negligible.

4.2 *Compensating PA Signals for Fluence Variation*

The PA response from an absorbing solution in tubes embedded in sample C [Fig. 1(a)] was measured following the procedure described in Sec. 3.3. The measured peak-to-peak values of PA signals from the tubes as a function of their depth along the optical axis [Fig. 1(c)], for both background scattering levels, are shown in Fig. 3(a). Since absorbers embedded in the medium with two levels of background scattering are identical and the same illumination and PA signal detection conditions are used, the variation in the PA signals from the absorbers at different depths is purely a result of fluence variations. In order to eliminate these, we measured the fluence variation in sample C along the line of absorbers [dotted line Fig. 1(c)], at the location of these tubes and in between with 0.5-mm step size, using our proposed method described earlier in Sec. 2. During the fluence measurements, the light is modulated with focused ultrasound transducer Panametrics: V310-su, 5 MHz. Figure 3(b) shows the measured decay in fluence as function of depth under the surface along the line of absorbers, when the sample is illuminated from the sides with background $\mu_s' = 6$ cm^{-1} and $\mu_s' = 10$ cm^{-1}, respectively. During the fluence measurements

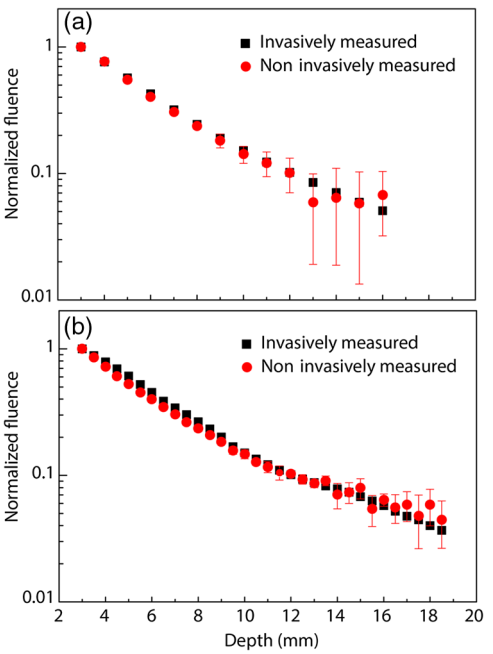

Fig. 2 Comparison of noninvasively measured (proposed method) against invasively measured normalized optical fluence. (a) Optically homogeneous sample A. (b) Optically inhomogeneous scattering sample B. Error bars are calculated using error propagation of the standard deviation in measured speckle contrast change.

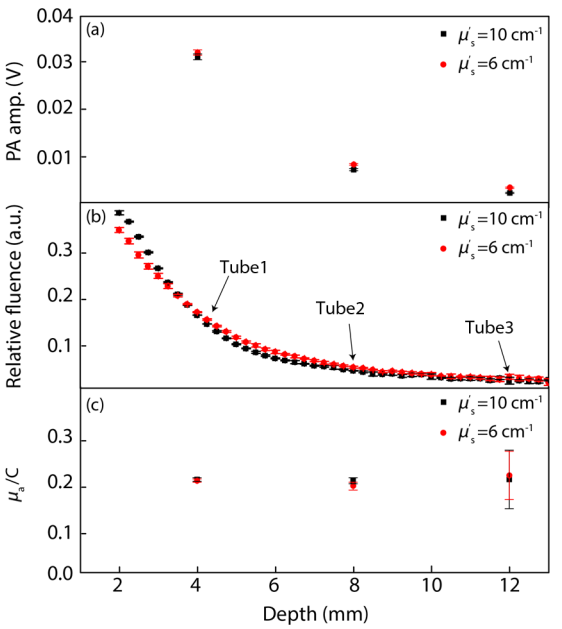

Fig. 3 Fluence compensation of PA signals. (a) Peak-to-peak value of PA signals from optically absorbing tubes. (b) Noninvasively measured relative fluence. (c) Fluence compensated PA signals (relative μa). The error bars on fluence compensated PA signals are based on the error propagation of the standard deviation of PA and fluence measurements.

in sample C, we used identical illumination aperture and wavelength as for PA measurements. Hence, the measured fluence decay has one-to-one correlation with the fluence decay during PA measurements. Therefore, by dividing the PA signal amplitudes plotted in Fig. 3(a) by the measured relative fluence at the locations of the tubes, we obtain the fluence-compensated PA signals.

The fluence-compensated PA signal peak-to-peak levels from all the tubes are plotted in Fig. 3(c) as function of their depth. A fluence variation of an order of magnitude in the PA signals is compensated with an accuracy of 6%, regardless of the background scattering in the medium.

5 Discussion

We presented a theoretical concept that describes a method to experimentally measure the local fluence inside highly scattering medium without a requirement of any a priori knowledge of optical properties. The concept uses photon path reversibility and local tagging of light with efficiency η, in scattering media. Based on this concept, an analytical expression, Eq. (4), is derived for the local optical fluence in terms of externally measured quantity (power of tagged light $P_{l,1}$) and the constants that are related to detection geometry (A_1, Ω_1), US focus (A_2), and the interaction between US and light (η). The concept of photon path reversibility as used here assumes that the photons reaching the tagging volume in the tissue in a certain direction are proportionally represented by the photons leaving the tagging volume in the opposite direction. This would hold true for the multiply scattered light that creates near-isotropic irradiance. The condition might differ in circumstances such as close to the light source, medium boundaries, and in the shadow of highly absorbing objects. This will be investigated in a future study along with the feasibility of the method in biological tissue.

In Sec. 3.2, we introduced a derived form of Eq. (4) to measure optical fluence using ultrasonic modulation of light for local tagging and detection of tagged light based on speckle contrast change. We made an assumption related to the light modulation efficiency η of the ultrasound and active frontal area A_2 of US focus. We assumed that light modulation efficiency η of the ultrasound is independent of optical scattering properties of the medium. We justified our assumption about η experimentally, by using a sample with three scattering levels covering a range of typical scattering in biological tissue. In our experimental results, an agreement between the fluence measurements in Fig. 2(b) in all three regions indirectly validates our assumption about η being constant for the given range of scattering coefficients: a dependence of η on the local scattering coefficient would have led to a discontinuity in the noninvasively measured fluence at the interfaces between the two layers with different scattering coefficients. This aspect was studied by Wang[24] and Sakadzic and Wang:[25] their theoretical model predicts a strong dependence of light modulation on the scattering coefficient for low ultrasound pressure (small particle displacement $\ll$1 nm), whereas for high ultrasound pressure (particle displacement of $>$1 nm) this dependence is negligible.[25] In our experiments, we chose biologically relevant range of scattering coefficients 60 to 150 cm^{-1} and an ultrasound pressure of $\cong$1 MPa at a frequency of 5 MHz, which corresponds to a larger particle displacement ($\cong$20 nm). This may explain our experimental observation of the tagging efficiency being independent of local scattering property of the medium.

In presented experiments, we choose an acoustically homogeneous medium ensuring that active frontal area A_2 of US focus remains constant during the scan. However, real biological tissue is inhomogeneous in regard to speed of sound and acoustic attenuation, which might affect the shape and size of the US focus. To address the issue of acoustic inhomogeneities, our group has recently shown that ultrasound wave front shaping guided by PA signal feedback can be used to accommodate acoustic inhomogeneities in biological tissue in order to regain a well-formed US focus for modulation of light.[26]

Next, we showed that results of measuring fluence can be used to correct PA signals for fluence variations. In this experiment, we used a sample that has absorbers mimicking blood vessels embedded in scattering medium with two scattering levels. The choice of embedding absorbers in different scattering background was to further verify our assumption about η being independent of local scattering properties. Since PA signals are the result of local absorption coefficient multiplied with fluence, when divided with measured fluence the dependence of η on local scattering would have resulted in two different sets of values of fluence-compensated PA signals in Fig. 3(c). The collapse of compensated PA signals in Fig. 3(c) regardless of the background scattering shows that the estimation of relative fluence is accurate and independent of local scattering property for a given range of scattering levels. The elimination of fluence dependence from PA signals might lead to the noninvasive quantification of chromophore concentrations. For instance, by considering a calibration approach with a known absorber[17] embedded in the sample, one can estimate the constant [Eq. (5)] related to experimental parameters. The calibration would require measurement of the PA response of a known absorber and relative fluence using Eq. (5) at the location of this absorber. This can then lead to estimation of the absorption coefficient of unknown absorbers at any depth.

6 Conclusion

We presented an analytical model that relates ultrasonically modulated light measured at boundary in reflection geometry to the local optical fluence inside the scattering medium. We performed experiments on tissue phantoms with biologically relevant optical properties to validate the concept as a strategy to measure fluence variations. In these experiments, we used focused ultrasound to tag the light addressing a region of interest in the scattering medium and measured the backscattered ultrasonically tagged light using a CCD camera. The agreement between relative fluence measurements performed using our method and the invasive method in Sec. 4.1 establishes the validity of the proposed method. The results presented in Sec. 4.2 show that the proposed method of measuring fluence variations can be combined with PAI to eliminate optical fluence-related artifacts from PA images, which may be related to the position of absorbers in medium or optical inhomogeneities of the medium. Through experiments, for both explicitly mapping fluence and its combination with photoacoustics, we showed that the method is capable of measuring fluence variations in biological tissue-like media. Similarly, noninvasively measuring fluence as demonstrated here can be combined with different optical techniques such as photodynamic therapy, fluorescence imaging, and DOT. Future research will focus on quantifying the tagging process and modeling the spatial distribution of the tagging in the ultrasound focus and estimation of its effective frontal area, which will lead to quantitative imaging

modalities. These aspects will be explored by modeling the AO phenomenon based on the combination of ultrasound and light transport simulations.

Acknowledgments

This research is supported by the Technology Foundation in the Netherlands (STW) under vici-grant 10831 and MIRA Institute of Biomedical Technology and Technical Medicine, University of Twente.

References

1. L. H. V. Wang and S. Hu, "Photoacoustic tomography: in vivo imaging from organelles to organs," *Science* **335**(6075), 1458–1462 (2012).
2. M. Heijblom et al., "Visualizing breast cancer using the Twente photoacoustic mammoscope: what do we learn from twelve new patient measurements?," *Opt. Express* **20**(11), 11582–11597 (2012).
3. S. G. Resink, A. C. Boccara, and W. Steenbergen, "State-of-the art of acousto-optic sensing and imaging of turbid media," *J. Biomed. Opt.* **17** (4), 040901 (2012).
4. Y. T. Lin et al., "Quantitative fluorescence tomography using a combined tri-modality FT/DOT/XCT system," *Opt. Express* **18**(8), 7835–7850 (2010).
5. T. D. O'Sullivan et al., "Diffuse optical imaging using spatially and temporally modulated light," *J. Biomed. Opt.* **17**(7), 071311 (2012).
6. A. Ishimaru, *Wave Propagation and Scattering in Random Media*, Academic Press, New York (1978).
7. J. Schafer and A. Kienle, "Scattering of light by multiple dielectric cylinders: comparison of radiative transfer and Maxwell theory," *Opt. Lett.* **33**(20), 2413–2415 (2008).
8. A. Liemert and A. Kienle, "Analytical solution of the radiative transfer equation for infinite-space fluence," *Phys. Rev. A* **83**(3), 039903 (2011).
9. A. E. Profio, "Light transport in tissue," *Appl. Opt.* **28**(12), 2216–2221 (1989).
10. W. Cong et al., "Modeling photon propagation in biological tissues using a generalized Delta-Eddington phase function," *Phys. Rev. E* **76**(5), 051913 (2007).
11. A. E. Profio and D. R. Doiron, "Transport of light in tissue in photodynamic therapy," *Photochem. Photobiol.* **46**(5), 591–599 (1987).
12. L. H. Wang, S. L. Jacques, and L. Q. Zheng, "Mcml—Monte-Carlo modeling of light transport in multilayered tissues," *Comput. Methods Prog. Biol.* **47**(2), 131–146 (1995).
13. G. D. Mahan et al., "Ultrasonic tagging of light: theory," *Proc. Natl. Acad. Sci. U. S. A.* **95**(24), 14015–14019 (1998).
14. B. Cox et al., "Quantitative spectroscopic photoacoustic imaging: a review," *J. Biomed. Opt.* **17**(6), 061202 (2012).
15. A. Rosenthal, D. Razansky, and V. Ntziachristos, "Quantitative optoacoustic signal extraction using sparse signal representation," *IEEE Trans. Med. Imaging* **28**(12), 1997–2006 (2009).
16. Z. Yuan and H. B. Jiang, "Quantitative photoacoustic tomography: recovery of optical absorption coefficient maps of heterogeneous media," *Appl. Phys. Lett.* **88**(23), 231101 (2006).
17. A. Q. Bauer et al., "Quantitative photoacoustic imaging: correcting for heterogeneous light fluence distributions using diffuse optical tomography," *J. Biomed. Opt.* **16**(9), 096016 (2011).
18. K. Daoudi et al., "Correcting photoacoustic signals for fluence variations using acousto-optic modulation," *Opt. Express* **20**(13), 14117–14129 (2012).
19. J. Li, G. Ku, and L. H. V. Wang, "Ultrasound-modulated optical tomography of biological tissue by use of contrast of laser speckles," *Appl. Opt.* **41**(28), 6030–6035 (2002).
20. Y. Z. Li et al., "Detection of ultrasound-modulated diffuse photons using spectral-hole burning," *Opt. Express* **16**(19), 14862–14874 (2008).
21. M. Gross et al., "Detection of the tagged or untagged photons in acousto-optic imaging of thick highly scattering media by photorefractive adaptive holography," *Eur. Phys. J. E* **28**(2), 173–182 (2009).
22. B. Jayet, J. P. Huignard, and F. Ramaz, "Optical phase conjugation in $Nd:YVO_4$ for acousto-optic detection in scattering media," *Opt. Lett.* **38**(8), 1256–1258 (2013).
23. S. G. Resink, E. Hondebrink, and W. Steenbergen, "Towards acousto-optic tissue imaging with nanosecond laser pulses," *Opt. Express* **22**(3), 3564–3571 (2014).
24. L. H. V. Wang, "Mechanisms of ultrasonic modulation of multiply scattered coherent light: an analytic model," *Phys. Rev. Lett.* **87**(4), 043903 (2001).
25. S. Sakadzic and L. H. V. Wang, "Ultrasonic modulation of multiply scattered coherent light: an analytical model for anisotropically scattering media," *Phys. Rev. E* **66**(2), 026603 (2002).
26. J. Staley et al., "Photoacoustic guided ultrasound wavefront shaping for targeted acousto-optic imaging," *Opt. Express* **21**(25), 30553–30562 (2013).

Biographies of the authors are not available.